EPJ Web of Conferences **276**, 02014 (2023) https://doi.org/10.1051/epjconf/202327602014
SQM 2022

Heavy-flavor jets in heavy-ion collisions

Saehanseul Oh[1,2,*]

[1]Sejong University, Seoul, South Korea
[2]Lawrence Berkeley National Laboratory, Berkeley, CA, USA

Abstract. Heavy-flavor jets are a unique tool to study dynamical evolution of QCD systems via heavy-flavor particles, allowing one to access to the original parton kinematics and to separate out production and fragmentation effects. In these proceedings, various heavy-flavor jet results in pp, pA, and AA collisions are presented, extending the scope of heavy-flavor studies discussed at this conference series, the Strangeness in Quark Matter.

1 Introduction

The measurement of heavy-flavor production has long been considered as one of the ideal probes to investigate the properties of the Quark-Gluon Plasma created in relativistic heavy-ion collisions. The large mass of charm (c) and bottom (b) quarks requires its production to occur at the early stage of the collision. This leads heavy quarks to interact with the medium as they traverse it, and to be sensitive to the transport properties of the medium. Recently, there have been significant efforts to study heavy-flavor jets, which can provide further information with respect to heavy-flavor single-hadron measurements. Heavy-flavor jets have better access to the original parton kinematics, and they enable to separate out production and fragmentation effects.

Jets themselves have been widely used to understand the interaction of hard-scattered partons with the quark-gluon plasma [1]. The study of heavy-flavor jets can particularly shed light on the dependence of jet-medium interaction on the parton flavor, which largely attributes to mass dependent effects and color-charge effects [2–5]. Compared to the inclusive jet measurements, the main complication in heavy-flavor jet measurements arises from how to identify heavy-flavor jets. There are mainly two distinguished methods, i) reconstructing jets first with jet reconstruction algorithm, e.g. anti-k_{T} algorithm [6], then using the properties of jet constituents, such as impact parameter of constituents or secondary vertex reconstructed with constituents, for identification of the original parton flavor [7], and ii) reconstructing heavy-flavor single-hadron first, then running the jet finding algorithm including the heavy-flavor hadron as a constituent, and identifying the jet containing the heavy-flavor hadron [8]. Each method has pros and cons considering statistics, kinematic limit in detectors, and identification purity. Heavy-flavor jets identified with method i) are referred to as c-jet or b-jet, and those with method ii) are D^0-jet or J/ψ-jet depending on the heavy-flavor hadron used for the identification.

*e-mail: saehanseul.oh@sejong.ac.kr

In these proceedings, selected heavy-flavor jet results are discussed including results in small collision systems, such as proton-pronton (pp) and proton-ion (pA) collisions, as well as in heavy-ion (AA) collisions.

2 Heavy-flavor jets in pp and pA collisions

Attributing to its large mass compared to the non-perturbative QCD scale ($\Lambda_{\rm QCD}$), heavy-quark production cross section has been calculated with the perturbative QCD framework [9–11]. In order to further test the validity of theoretical predictions and to provide constraints on perturbative QCD calculations, a variety of heavy-flavor jet cross-section measurements have been performed in pp collisions at several center of mass energies from different experiments at the LHC [8, 12–16]. Figure 1 shows cross-section ratios of D^0-jets to inclusive jets [15] (left), and of b-jets to inclusive jets [16] (middle) in $\sqrt{s}$ = 5.02 TeV pp collisions reported by ALICE and ATLAS Collaborations, respectively. Throughout the $p_{\rm T,jet}$ range, which is significantly different in two results, the ratios agree well with the PYTHIA 8 predictions, while the POWHEG + PYTHIA 8 calculations are observed to slightly disagree with the data at low $p_{\rm T,jet}$.

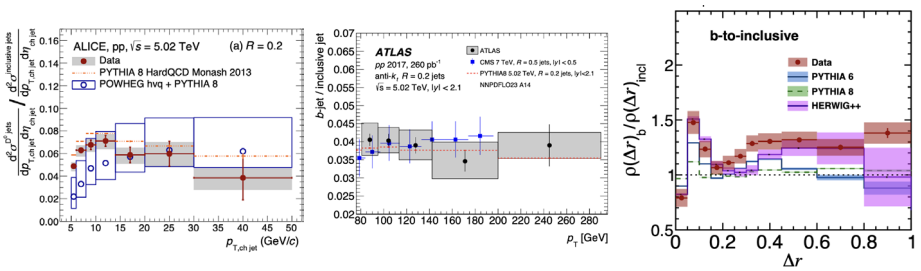

Figure 1. Cross-section ratios of D^0-jets to inclusive charged-particle jets [15] (left) and of b-jets to inclusive jets [16] (middle). b-to-inclusive jet shape ratio as a function of radial distance from the jet axis (Δr) with $p_{\rm T,jet} > 120$ Ge$/c$ and $p_{\rm T,trk} > 1$ GeV$/c$ is shown on the right panel [17]. All results are from pp collisions at $\sqrt{s}$ = 5.02 TeV.

In addition to the cross-section measurements, several other observables for heavy-flavor jets have been measured in pp collisions, not only providing constraints to theoretical calculations, but also serving as a baseline for the corresponding measurements in heavy-ion collisions. The right panel in Fig. 1 presents the b-to-inclusive jet shape ratio as a function of radial distance, Δr, with respect to the jet axix for jets with $p_{\rm T,jet} > 120$ Ge$/c$ and $p_{\rm T,trk} > 1$ GeV$/c$ [17]. The result indicates a shift of transverse momentum from small to large radial distance for b-jets compared to inclusive jets, and it gives a hint of the dead cone effect, which predicts the suppression of radiation from an emitter of mass m and energy E in the angular region, $\theta \leq m/E$ [18].

Furthermore, the dead cone effect in QCD has been directly observed using D^0-jets and experimental declustering techniques [19]. The observable of this measurement is defined by the ratio of the splitting angle (θ) distributions for D^0-jets to inclusive jets in bins of $E_{\rm Radiator}$,

$$R = \frac{1}{N^{D^0\rm jet}} \frac{{\rm d}n^{D^0\rm jet}}{{\rm d}\ln(1/\theta)} \Big/ \frac{1}{N^{\rm inclusivejet}} \frac{{\rm d}n^{\rm inclusivejet}}{{\rm d}\ln(1/\theta)} \Big|_{k_{\rm T},E_{\rm Radiator}},$$

where θ, $k_{\rm T}$, and $E_{\rm Radiator}$ are the splitting angle between two prongs, relative transverse momentum of the splitting, and sum of the energy of two prongs at each declustering step, re-

spectively. In Fig. 2, a significant suppression in the rate of small-angle splittings is observed in D^0-jets with respect to inclusive jets, which directly contrasts to the no dead-cone limit from theoretical calculations. The suppression magnitude increases with decreasing E_{Radiator}, agreeing with the expectation from the equation for dead-cone effect region, $\theta \leq m/E$.

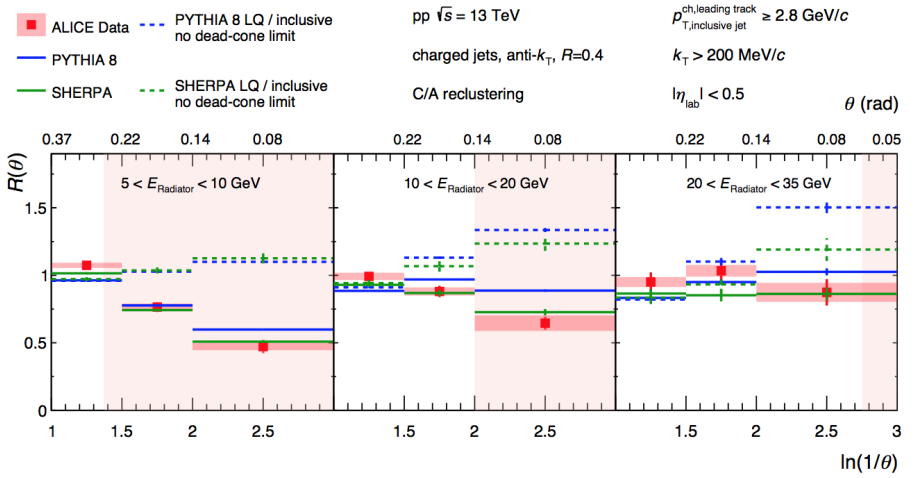

Figure 2. Ratios of the splitting-angle probability distributions for D^0 jets to inclusive jets in $\sqrt{s}$ = 13 TeV pp collisions with 5 < E_{Radiator} < 10 GeV (left), 10 < E_{Radiator} < 20 GeV (middle), and 20 < E_{Radiator} < 35 GeV (right) [19]. No dead-cone limit from event generators are shown with dashed lines.

Heavy-flavor jet cross section measurements have also been performed in pA collisions to investigate contributions of cold nuclear matter effects on jet production and jet quenching in heavy-ion collisions [21]. Figure 3 shows results of nuclear modification factor in pA collisions, $R_{p\text{A}}$, i.e. the ratio of cross section in pA collisions to that in pp collisions scaled by the ion mass number, with c-jets (left) and b-jets (middle and right) [14, 22, 23]. The $R_{p\text{A}}$ value with its uncertainties demonstrates no significant jet modification in p-Pb collisions at $\sqrt{s_{\text{NN}}}$ = 5.02 TeV. This leads to the conclusion that cold nuclear matter effects do not play a significant role in jet energy modification in heavy-ion collisions in the corresponding collision energy.

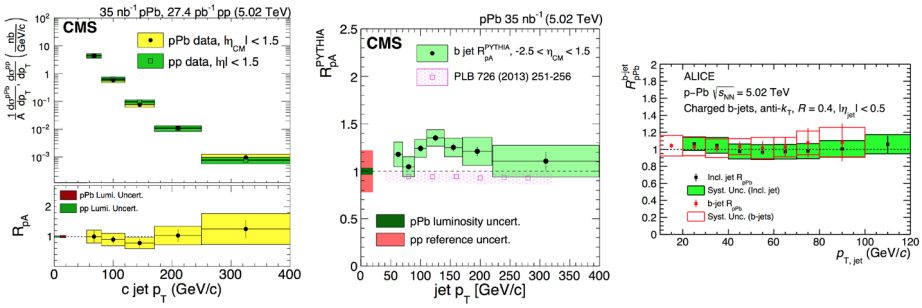

Figure 3. Cross-section and $R_{p\text{A}}$ with c-jets [23] (left) and $R_{p\text{A}}$ with b-jets (middle and right) [14, 22] in $\sqrt{s_{\text{NN}}}$ = 5.02 TeV p-Pb collisions.

3 Heavy-flavor jets in AA collisions

With baseline results in pp and pA collisions, heavy-flavor jets are measured in heavy-ion collisions in order to study the parton flavor dependence of jet quenching. The nuclear modification factor, $R_{\rm AA}$, indicates the deviation of inclusive spectra in heavy-ion collisions with respect to those in pp collisions, and is defined as

$$R_{\rm AA} = \frac{\frac{1}{N_{\rm event}}(\mathrm{d}^2 N_{\rm AA})/(\mathrm{d}p_{\rm T}\,\mathrm{d}\eta)}{\langle T_{\rm AA}\rangle(\mathrm{d}^2\sigma_{pp})/(\mathrm{d}p_{\rm T}\,\mathrm{d}\eta)},$$

where $N_{\rm AA}$, $\sigma_{\rm pp}$, and $T_{\rm AA}$ corespond to the yield in AA collisions, corss section in pp collisions, and the nuclear overlap function, respectively. Figure 4 shows $R_{\rm AA}$ of b-jets [16]

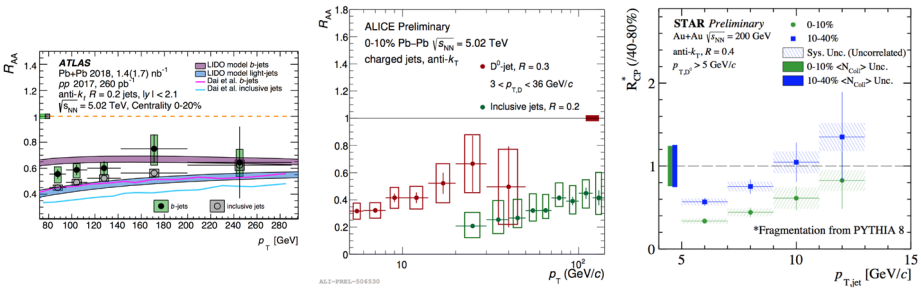

Figure 4. $R_{\rm AA}$ for b-jets and inclusive jets in 0–20% central collisions [16] (left), and for D^0-jets and inclusive jets in 0-10% central collisions [24] in $\sqrt{s_{\rm NN}}$ = 5.02 TeV Pb+Pb collisions at the LHC, and $R_{\rm CP}$ for D^0-jets in $\sqrt{s_{\rm NN}}$ = 200 GeV Au+Au collisions at RHIC (right) [25].

(left) and D^0-jets [24] (middle) in Pb+Pb collisions at $\sqrt{s_{\rm NN}}$ = 5.02 TeV, and $R_{\rm CP}$, nuclear modification factor with respect to peripheral heavy-ion collisions instead of pp collisions, in Au+Au collisions at $\sqrt{s_{\rm NN}}$ = 200 GeV [25]. Although only the most central collision results (0–20%) are presented at $\sqrt{s_{\rm NN}}$ = 5.02 TeV due to the page limit in these proceedings, the $R_{\rm AA}$ values of b-jets and inclusive jets show a gradual decrease in more central collisions, and $R_{\rm CP}$ results follow the similar trend. In central collisions, both b-jets and D^0-jets have larger $R_{\rm AA}$ values compared to those of inclusive jets. These results along with theoretical predictions provide a hint that the difference may attribute to larger gluon contribution in inclusive jet sample, as gluon jets are expected to lose more energy than quark jets. However, the current systematic uncertainties do not allow more definitive conclusion.

There have also been measurements regarding internal structure of heavy-flavor jets, such as jet shape, fragmentation function, and radial profile of heavy-flavor meson within jets [25–28]. Among such results, the radial distributions of D^0 meson within D^0-jets in pp and Pb+Pb collisions are shown in Fig. 5. These distributions are sensitive not only to the production mechanisms of the meson, but also to the energy loss and diffusion processes in the interaction between parton and hot QCD medium created in heavy-ion collisions. In Pb+Pb collisions, the D^0 meson distribution for low transverse momentum ($4 < p_{\rm T}^{D^0} < 20$ GeV/c) is enhanced at a larger distance with respect to the jet axis compared to the corresponding result in pp collisions, and this is an indication of charm quark diffusion in heavy-ion collisions. On the other hand, this modification is not observed at higher transverse momentum ($p_{\rm T}^{D^0} > 20$ GeV/c), and the overall results well agree with the CCNU energy loss model [29]. Such results as well as other heavy-flavor jet internal structure measurements provide constraints on physics mechanisms relevant to the heavy quark propagation inside the quark gluon plasma.

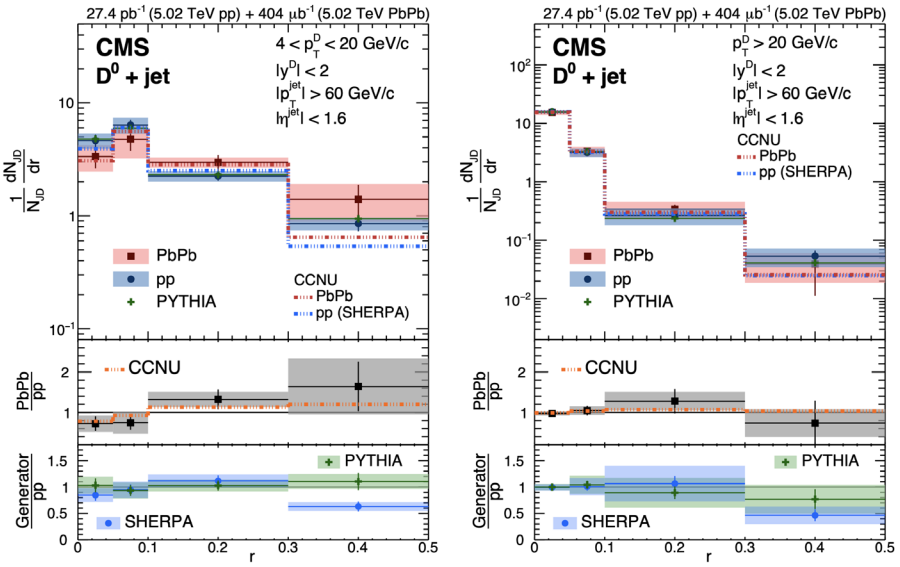

Figure 5. Radial distributions of D^0 mesons within D^0-jets in pp and Pb+Pb collisions at $\sqrt{s_{\rm S}}$ = 5.02 TeV. r is defined by the radial distance between D^0 meson and the jet axis. D^0-jets have $p_{\rm T,jet}$ larger than 60 GeV/c, and D^0 mesons are selected with $4 < p_{\rm T}^{D^0} < 20$ GeV/c (left) and $p_{\rm T}^{D^0} > 20$ GeV/c [28].

Heavy-flavor jet measurements are one of the key points where the upcoming LHC Run 3 and 4, as well as sPHENIX and STAR runs in years of 2023-2025 will play a crucial role with significantly larger statistics and improved detector performances. Different kinematic ranges from different experiments can provide comprehensive picture of the flavor dependence of jet quenching, for example, verifying the statement that low-$p_{\rm T,jet}$ results are more sensitive to mass-dependent effects.

References

[1] G.-Y. Qin and X.-N. Wang, Int. J. Mod. Phys. E **24**, 1530014 (2015)
[2] H. van Hees, R. Rapp, Phys. Rev. C **71**, 034907 (2005)
[3] G. D. Moore, D. Teaney, Phys. Rev. C **71** 064904 (2005)
[4] S. Wang, W. Dai, B.-W. Zhang, E. Wang, Eur. Phys. J. C **79**, 789 (2019)
[5] Y. L. Dokshitzer, D. E. Kharzeev, Phys. Lett. B **519**, 199 (2001)
[6] M. Cacciari, G. P. Salam, and G. Soyez, JHEP **04**, 063 (2008)
[7] CMS Collaboration, JINST **8**, P04013 (2013)
[8] ALICE Collaboration, JHEP **1908** (2019) 133
[9] J.C. Collins, D.E. Soper, Annu. Rev. Nucl. Part. Sci. **37**, 383 (1987)
[10] S. Frixione, M. L. Mangano, P. Nason, G. Ridolfi, Adv. Ser. Direct. High Energy Phys. **15**, 609–706 (1998)
[11] M. Cacciari, M. Greco, P. Nason, JHEP **05**, 007 (1998)
[12] CMS Collaborartion, JHEP **04**, 084 (2012)
[13] ATLAS Collaboration, Eur. Phys. J. C **71**, 1846 (2011)
[14] ALICE Collaboration, JHEP **01**, 178 (2022)

[15] ALICE Collaboration, arXiv:2204.10167, submitted to JHEP (2022)
[16] ATLAS Collaboration, arXiv:2204.13530, submitted to Eur. Phys. J. C (2022)
[17] CMS Collaboration, JHEP **05**, 054 (2021)
[18] Y. L. Dokshitzer, V. A. Khoze, S. I. Troian, J. Phys. G **17**, 1602-1604 (1991)
[19] ALICE Collaboration, Nature **605**, 7910, 440–446 (2022)
[20] ALICE Collaboration, Phys. Lett. B **827**, 136984 (2022)
[21] C. A. Salgado et al., J. Phys. G **39**, 015010 (2012)
[22] CMS Collaborartion, Phys. Lett. B **754**, 59 (2016)
[23] CMS Collaborartion, Phys. Lett. B **772**, 306 (2017)
[24] M. Mazzilli (for the ALICE Collaboration), arXiv:2208.10908, Quark Matter 2022 proceedings (2022)
[25] D. Roy (for the STAR Collaboration), arXiv:2207.14434, Quark Matter 2022 proceedings (2022)
[26] X. Wang (for the CMS Collaboration), Quark Matter 2022 (2022)
[27] CMS Collaboration, Phys. Lett. B **825**, 136842 (2021)
[28] CMS Collaboration, Phys. Rev. Lett. **125**, 102001 (2020)
[29] S. Wang, W. Dai, B.-W. Zhang, E. Wang, Eur. Phys. J. C **79** 789 (2019)